Supporting Information

Understanding the Microwave Heating Properties of La-Ce-Ni Oxides Based on Structural, Dielectric, and Conductive Analysis

Tatsuya Hamashima[1], Masateru Nishioka[2], Takeharu Sugiyama[3], Ken Watanabe[4], Hajime Hojo[4], and Hisahiro Einaga[4,*]

1 Department of Interdisciplinary Engineering Sciences, Interdisciplinary Graduate School of Engineering Sciences, Kyushu University, Fukuoka 816-8580, Japan.
2 Minamo corporation, Miyagi 989-3127, Japan.
3 Kyushu University Synchrotron Light Research Center, Kyushu University, 6-1, Kasugakoen, Kasuga, Fukuoka 816-8580, Japan.
4 Department of Advanced Materials Science and Engineering, Faculty of Engineering Sciences, Kyushu University, Fukuoka 816-8580, Japan.

e-mail: einaga.hisahiro.399@m.kyushu-u.ac.jp

2.1 Experimental section

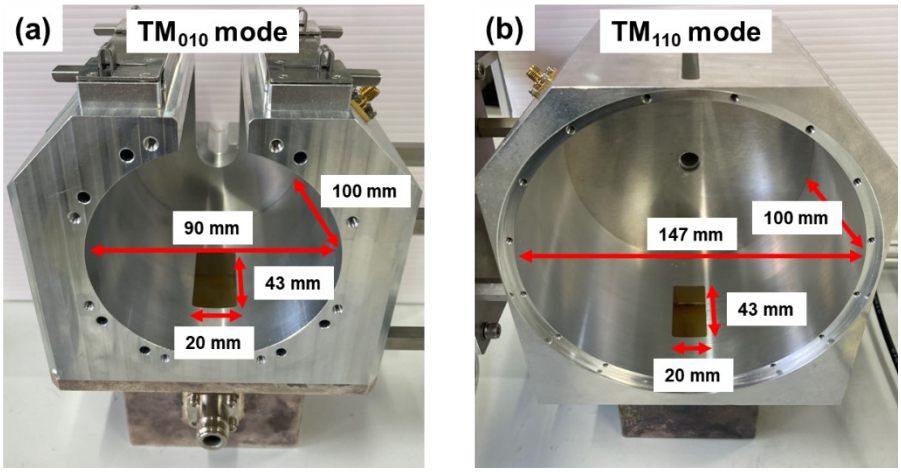

Figure S1. Images of the cavity resonator for (a)TM010 mode and (b)TM110 mode

A cylindrical single-mode cavity resonator with an inner diameter of 90 mm and a length of 100 mm, made of aluminum is TM010 mode for electric field heating and with an inner diameter of 147 mm and a length of 100 mm, made of aluminum is TM110 mode for magnetic field heating. A coaxial waveguide adapter was coupled via a 20 mm 43 mm wide iris for each resonator.

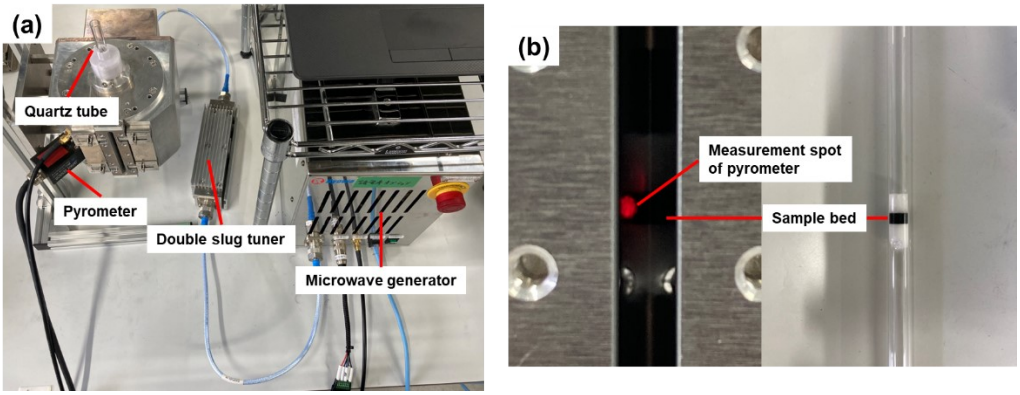

Figure S2. (a) Image of microwave heating setup and (b) close-up view of the sample bed

The quartz tube with the samples was surely placed at the central axis of the resonator, and sample was located at the middle of the resonator, matching the measurement spot of the infrared pyrometer.

3.1 Material characterization

Table S1. Crystallite sizes of $LaNiO_3$ phase estimated from the diffraction peak near $2\theta = 23^o$ and CeO_2 phase from the peak near $2\theta = 28^o$, using the Scherer equation

Sample	$LaNiO_3$ phase (nm)	CeO_2 phase (nm)
Ce/La = 0	28	n.d.
Ce/La = 1/9	20	15
Ce/La = 2/8	17	19
Ce/La = 3/7	16	17
Ce/La = 4/6	17	18
Ce/La = 5/5	8	23

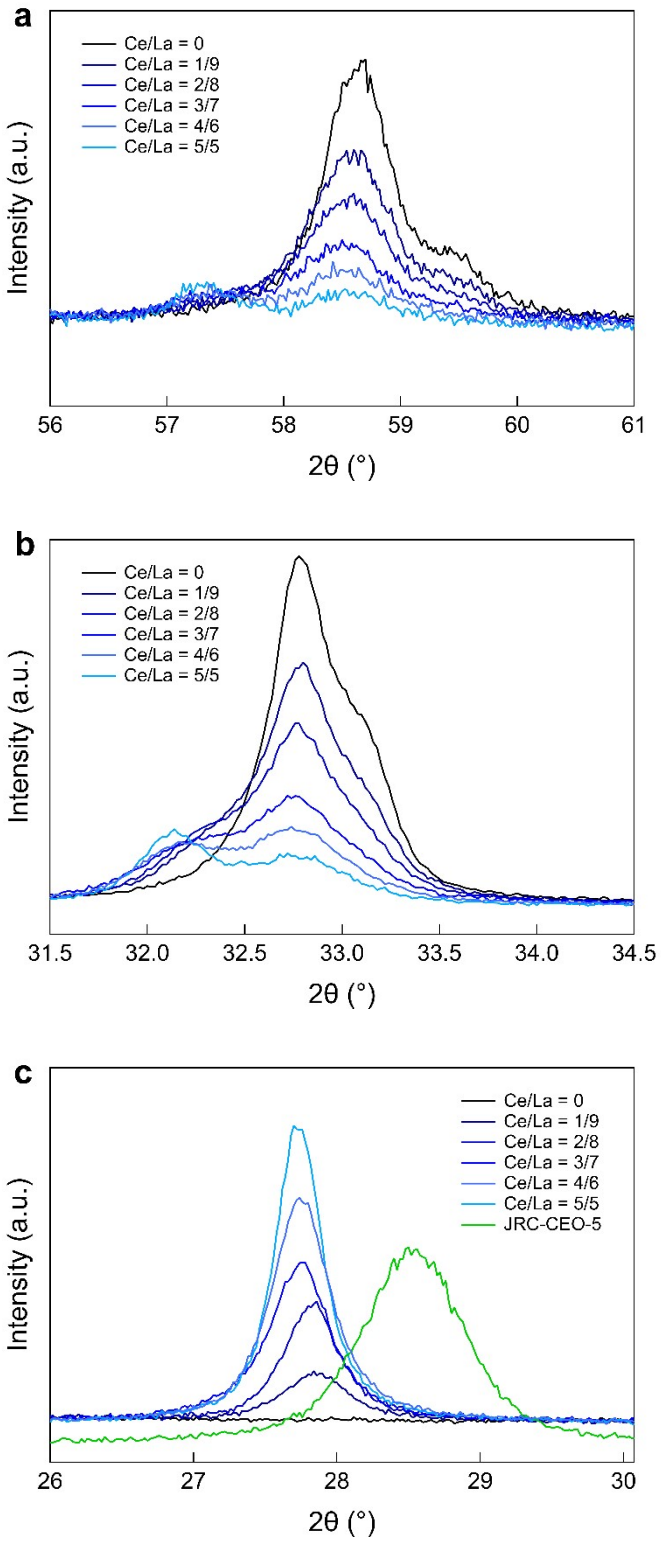

Figure S3. XRD peak corresponding to (a) $LaNiO_3$ phase near 2θ = 59°, (b) $LaNiO_3$ phase near 2θ = 33°, and (c) CeO_2 phase near 2θ = 28°

Table S2. Ni K-edge X-ray absorption edge energies of La-Ce-Ni oxides

Sample	Absorption edge (eV)
Ce/La = 0	8345.1
Ce/La = 1/9	8344.5
Ce/La = 2/8	8344.0
Ce/La = 3/7	8343.4
Ce/La = 4/6	8343.1
Ce/La = 5/5	8342.7

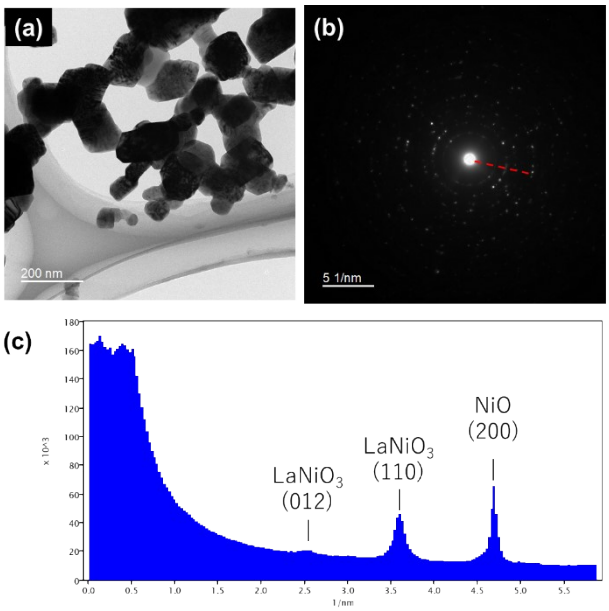

Figure S4. (a) Bright-field TEM image, (b) Electron diffraction pattern, and (c) Intensity profile of the electron diffraction along the red-dotted line ($LaNiO_3$)

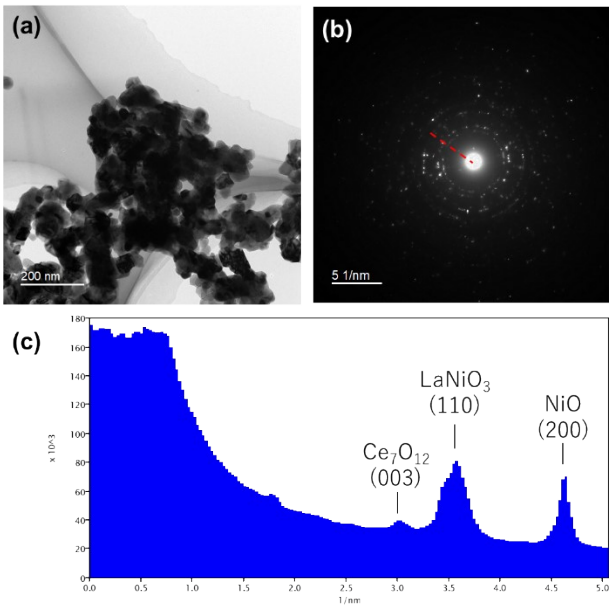

Figure S5. (a) Bright-field TEM image, (b) Electron diffraction pattern, and (c) Intensity profile of the electron diffraction along the red-dotted line ($La_{0.7}Ce_{0.3}NiO_3$)

The crystal planes of each phase were determined by calculating the interplanar spacings from the diffraction patterns and comparing them with the reference diffraction data taken from ICDD PDF2 ($LaNiO_3$: PDF# 01-079-2451, NiO: PDF# 00-047-1049, Ce_7O_{12}: PDF# 01-071-567)

Table S3. Specific surface area of La-Ce-Ni oxides

Sample	S_{BET} (m^2/g)
Ce/La = 0	5.0
Ce/La = 1/9	6.1
Ce/La = 2/8	10.6
Ce/La = 3/7	8.4
Ce/La = 4/6	9.4
Ce/La = 5/5	9.6

3.2 Heating Properties of Samples Under Electric Field

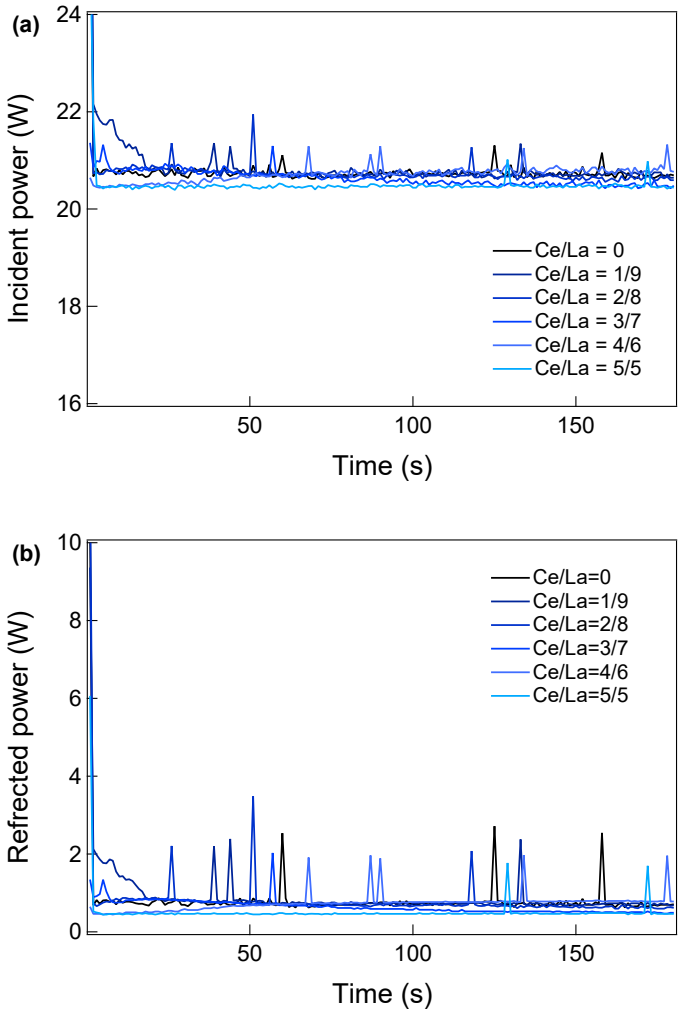

Figure S6. (a)Incident and (b)reflected microwave power under microwave electric field

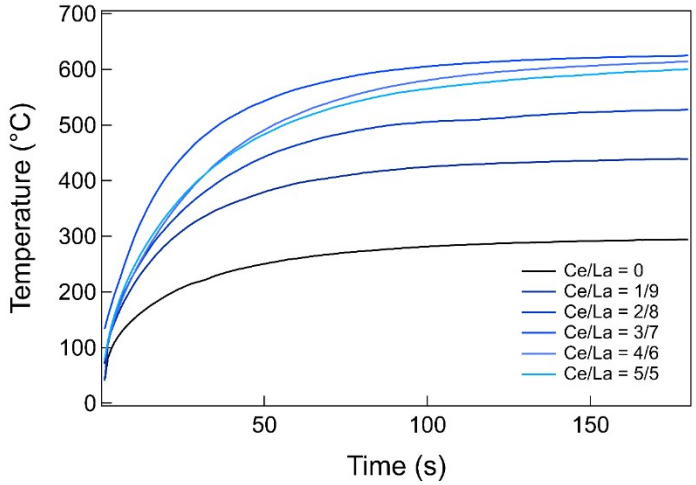

Figure S7. Temperature profiles of La-Ce-Ni oxides under microwave electric field heating at 20 W

Table S4. Average heating rates of La-Ce-Ni oxides during the first 25 seconds under microwave electric field heating from room temperature

Sample	Heating rate (K/min)
Ce/La = 0	458
Ce/La = 1/9	714
Ce/La = 2/8	703
Ce/La = 3/7	1046
Ce/La = 4/6	857
Ce/La = 5/5	869

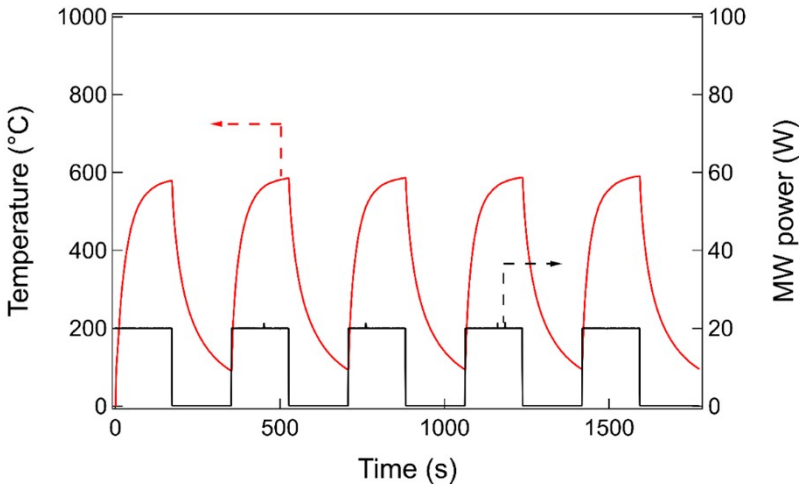

Figure S8. Reproducibility of heating properties of Ce/La = 3/7 under a microwave electric field at 20 W

Table S5. Average heating rates of La-Ce-Ni oxides during the first 25 seconds under microwave electric field heating at 15 W and 25 W from room temperature

Sample	Heating rate at 15 W (K/min)	Heating rate at 25 W (K/min)
Ce/La = 0	254	379
Ce/La = 3/7	628	986

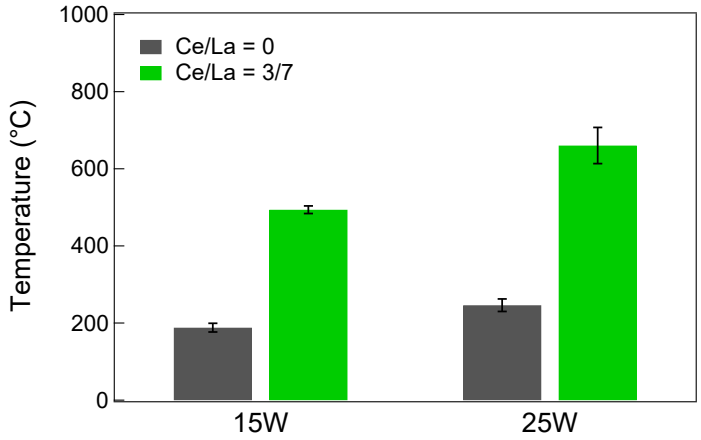

Figure S9 . Steady-state temperature after 3 minutes under microwave electric field heating at 15 W and 25 W

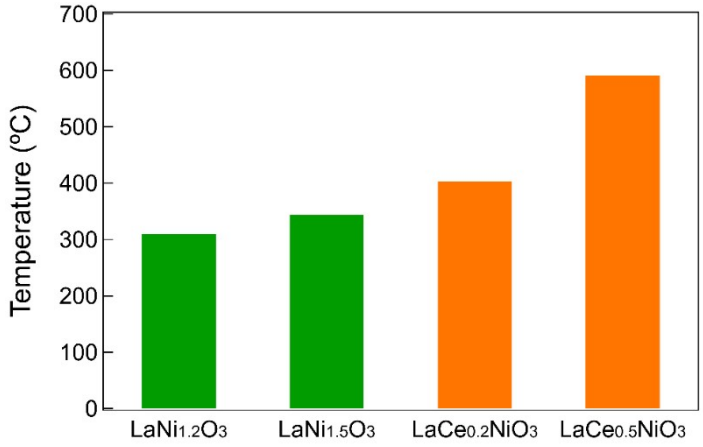

Figure S10. Steady-state temperature of catalysts with excess Ni and Ce after 3 minutes under microwave electric field at 20 W

The XRD pattern of the physically mixed sample is shown in Figure S6. The peak positions remain unchanged compared to La/Ce = 0 and JRC-CEO-5. The crystallite size of the $LaNiO_3$ phase, estimated from the peak around $2\theta = 23^{o}$, was 34 nm, which is even larger than La/Ce = 0; however, as previously discussed, it is not directly related to the heating properties.

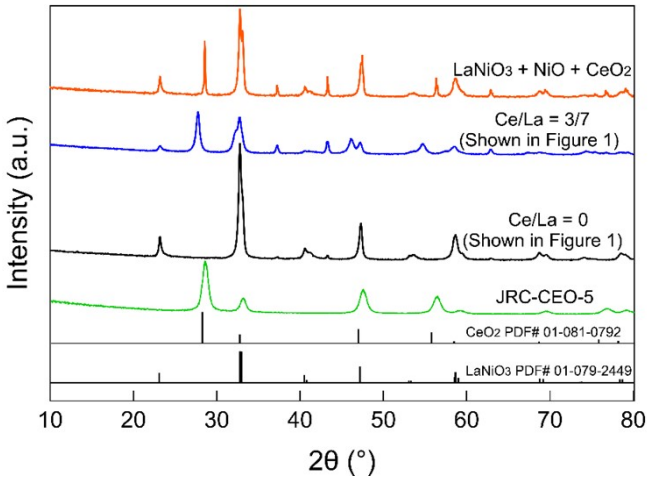

Figure S11. XRD patterns of the physically mixed sample, along with Ce/La = 3/7, Ce/La = 0, and JRC-CEO-5 as references

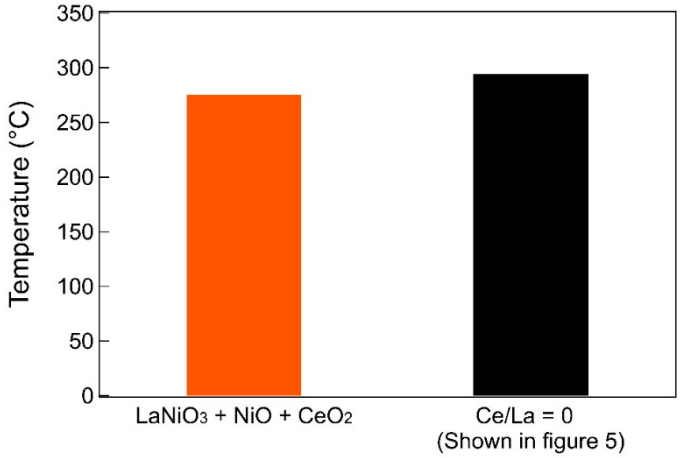

Figure S12. Steady-state temperature of $LaNiO_3$ mixed with NiO and CeO_2 under microwave electric field heating at 20 W of microwave power

The XRD pattern of the ball-milled sample is shown in Figure S8. The peak positions remain unchanged compared to the sample before ball milling, indicating that the crystal structure was preserved. However, the peak intensities decreased, and the crystallite size of $LaNiO_3$ phase is reduced from 28 nm to 14 nm.

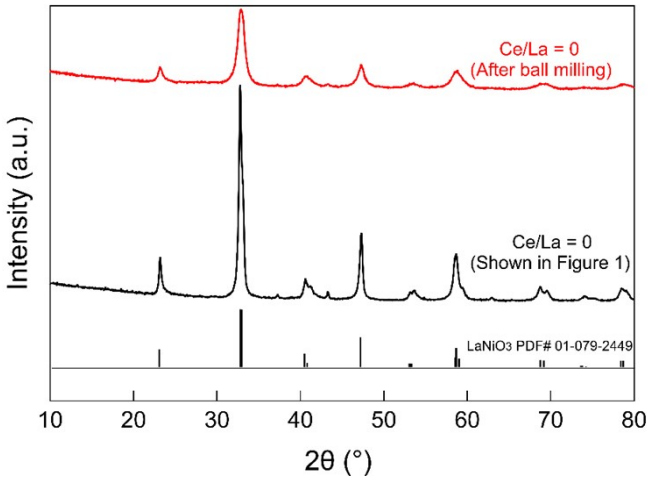

Figure S13. XRD pattern of the ball-milled sample, along with Ce/La = 0 as a reference

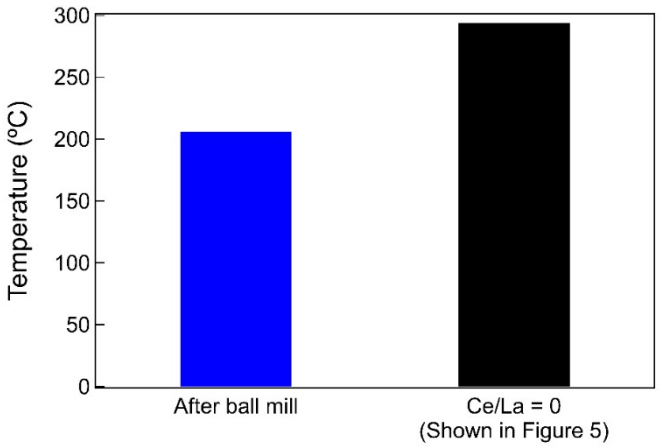

Figure S14. Steady-state temperature of the ball-milled sample under microwave electric field heating at 20 W of microwave power

3.3 Dielectric Properties of Samples

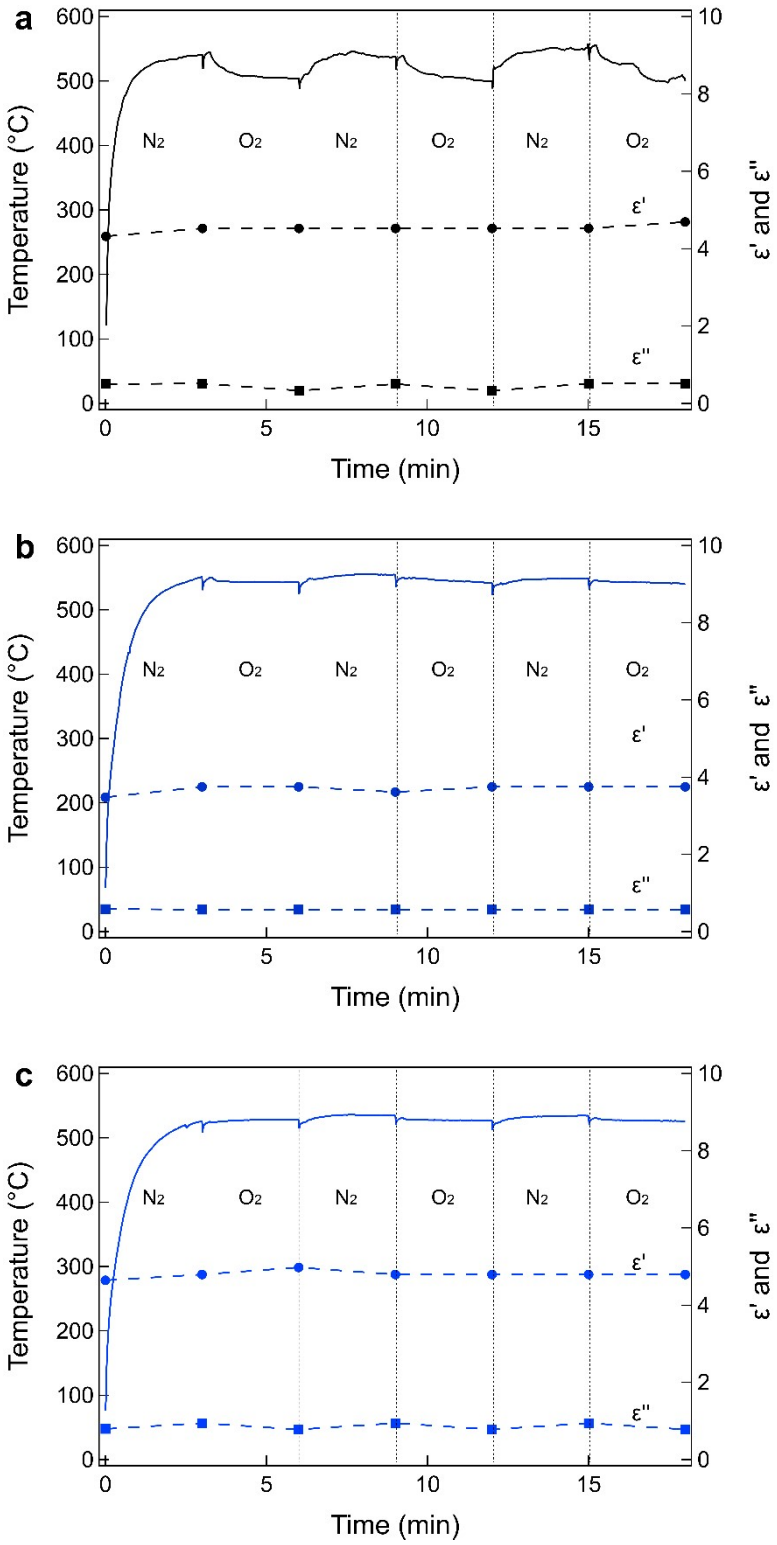

Figure S15. Temperature profile and dielectric properties of (a) Ce/La = 0, (b) Ce/La = 2/8, and (c) Ce/La = 3/7 under O_2 and N_2 flow

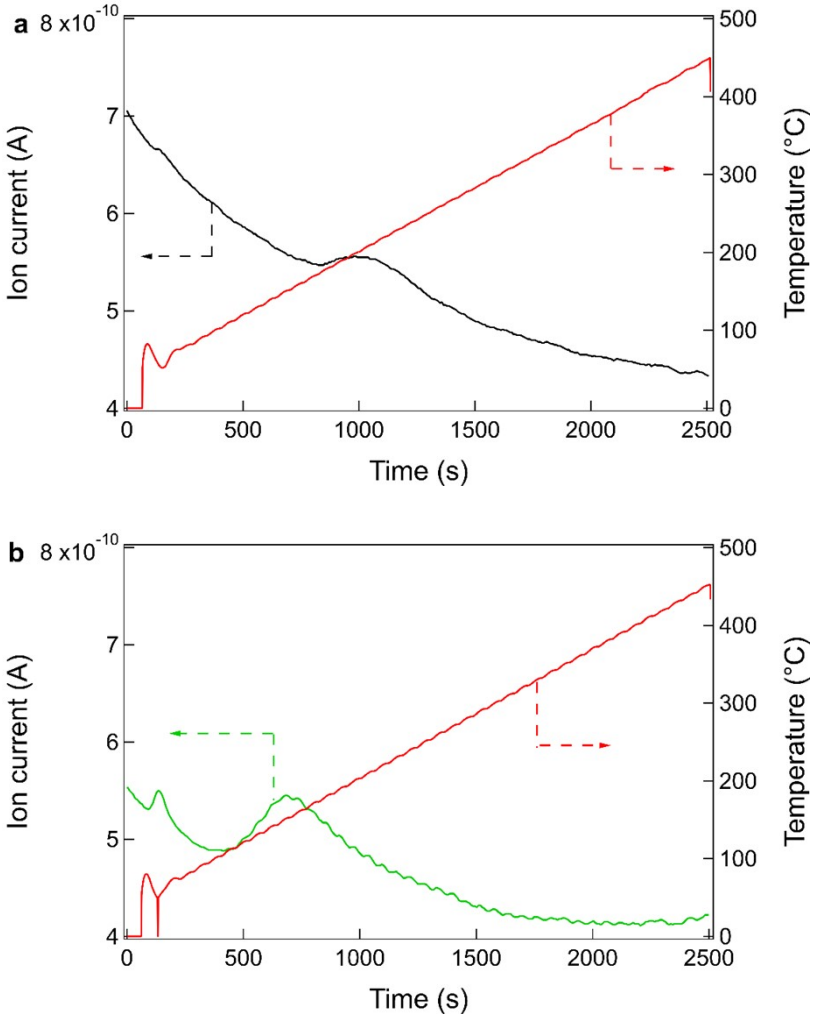

Figure S16. MS signals and the sample temperature profiles of (a) Ce/La = 0, and (b) Ce/La = 3/7 during O_2-TPD under microwave heating. The samples were first heated to 450 °C under an air flow, cooled to room temperature, and then reheated up to 450 °C under N_2 flow.

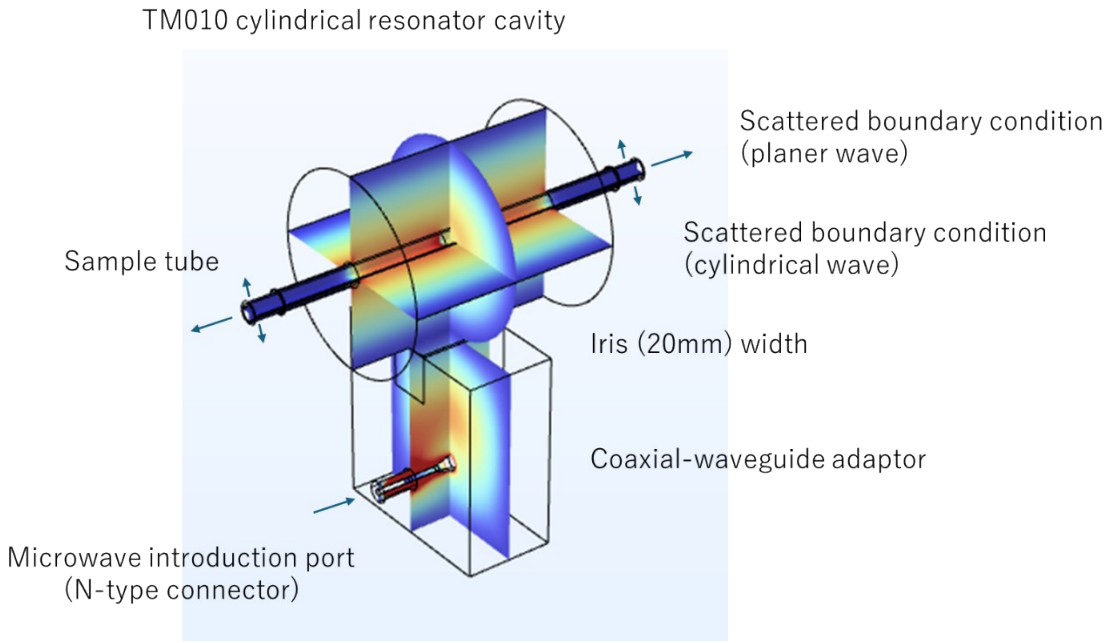

Figure S17. A proportional model of TM010 mode microwave reactor constructed using simulation software.

A TM010 cylindrical resonator cavity (90 mm diameter) and a coaxial waveguide adapter were coupled via a 20 mm wide iris. The boundary conditions for the simulations were as follows: All boundaries, except for the sample tube ends, were assumed to be perfect electric conductor (PEC) walls. The tube ends were modeled with a scattering boundary condition (SBC) that accounts for both cylindrical waves on the circumferential surface and planar waves on the flat ends of the cylinder. Microwave power was introduced from a coaxial port (designed as an N-type connector).

During practical microwave heating, the lack of perfect impedance matching causes reflected waves, and a small amount of microwave leakage can be observed from the viewing window. Accordingly, it must be recognized that the conditions differ to some extent from those in the simulation.

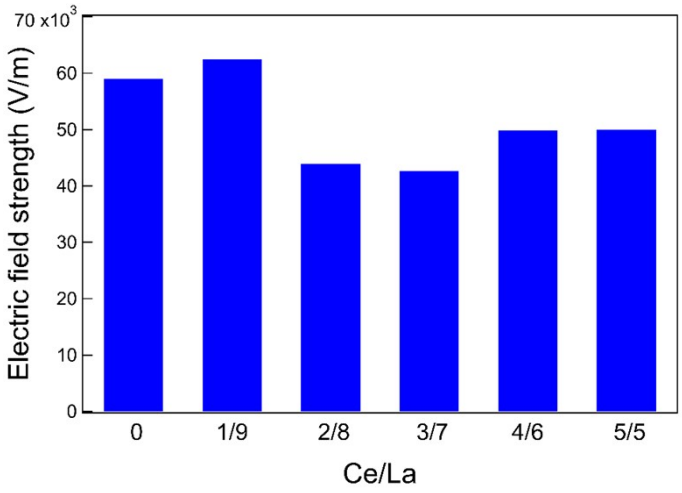

Figure S18. Simulated average electric field strength within the catalyst bed

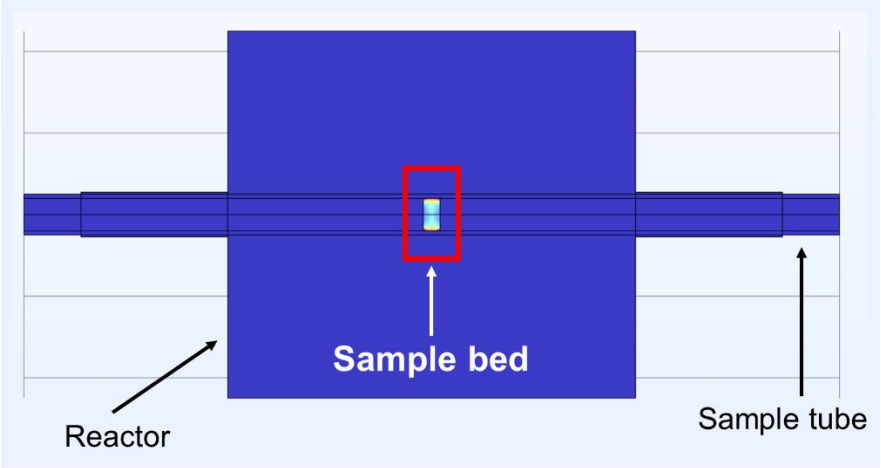

Figures S19. Simulated power loss density observed from the top-down view of the model, with the sample bed located at the center of the reactor

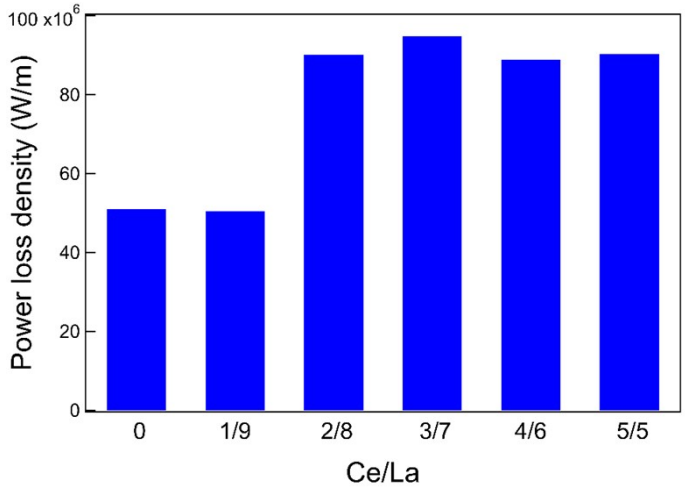

Figure S20. Simulated average power loss density within the catalyst bed

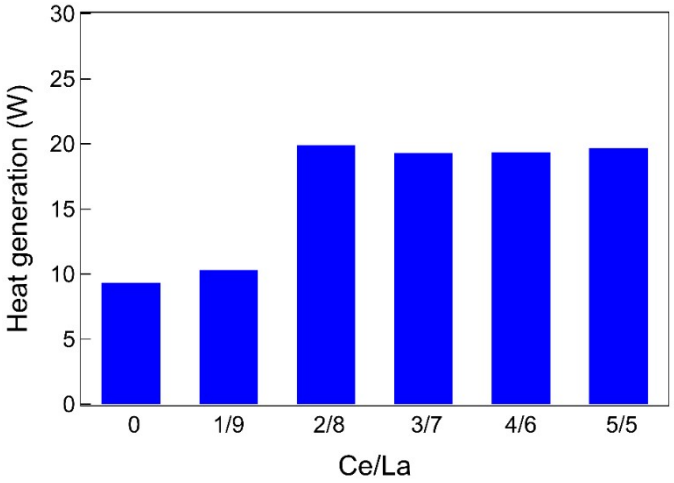

Figure S21. Simulated heat generation from the catalyst bed

3.4 Conductivity of Samples

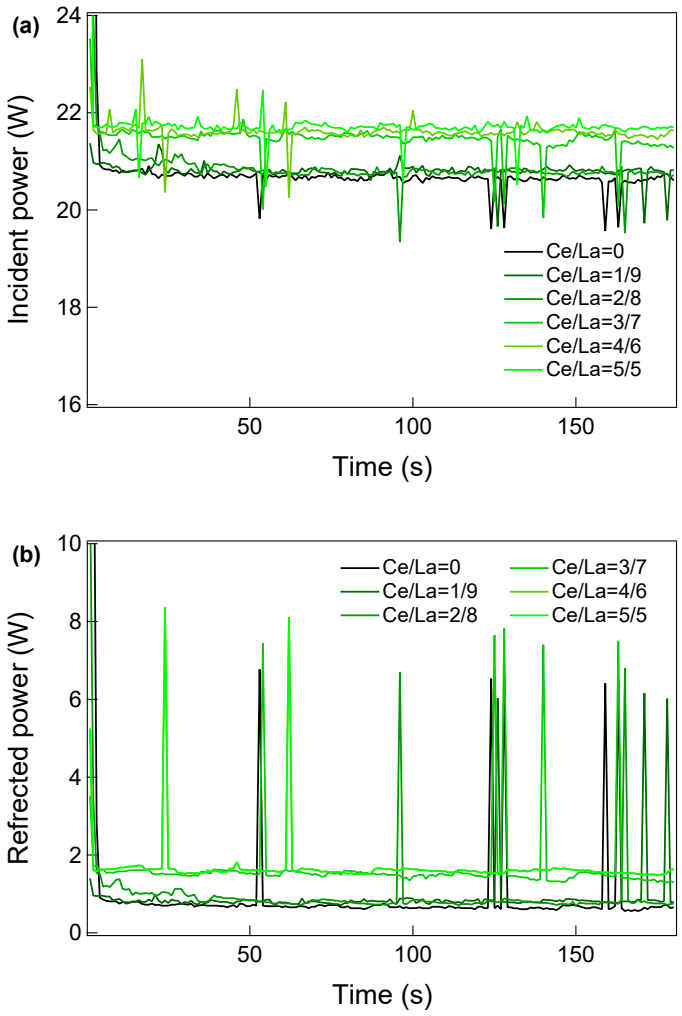

Figure S22. (a)Incident and (b)reflected microwave power under microwave magnetic field

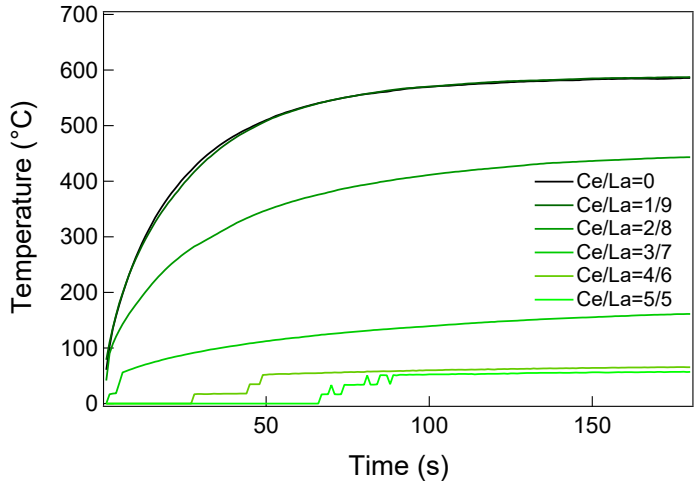

Figure S23. Temperature profiles of La-Ce-Ni oxides under microwave magnetic field heating at 20 W

Table S6. Average heating rates of La-Ce-Ni oxides during the first 25 seconds of microwave magnetic field heating from room temperature

Sample	Heating rate (K/min)
Ce/La = 0	956
Ce/La = 1/9	932
Ce/La = 2/8	613
Ce/La = 3/7	161
Ce/La = 4/6	n.d.
Ce/La = 5/5	n.d.

n.d.: not detected under the detection limit of the thermometer.